

# A magnetically actuated anchoring system for a wireless endoscopic capsule

Hao Zhou<sup>1</sup> · Gursel Alici<sup>1</sup>  · Fredy Munoz<sup>1</sup>

Published online: 27 October 2016  
© Springer Science+Business Media New York 2016

**Abstract** In this study, we propose a new magnetically actuated anchoring system for wireless capsule endoscopes (WCE) by employing the principle of a switchable magnetic spring. A force model is derived to predict the magnetic force needed to support the interaction between the anchors and the intestinal lumen. The theoretical and experimental analysis conducted shows that the magnetic spring is capable of providing the force needed to activate the anchoring mechanism, which consists of four foldable legs. A prototype capsule with a size comparable with the size of a commercial WCE was designed, fabricated, and tested. The *in-vitro* tests with a real small intestine show that the proposed anchoring mechanism is able to raise the friction force between the anchoring legs and inner wall of the intestine by more than two times after its activation using an external magnetic field. Experimental results presented demonstrate that the proposed anchoring system, which has a low foot-print not taking up too much space on the capsule, can provide a reliable anchoring capability with the capsule inside the intestinal lumen.

**Electronic supplementary material** The online version of this article (doi:10.1007/s10544-016-0129-0) contains supplementary material, which is available to authorized users.

✉ Gursel Alici  
gursel@uow.edu.au

Hao Zhou  
hzhou@uow.edu.au

Fredy Munoz  
ffm517@uow.edu.au

<sup>1</sup> School of Mechanical, Materials and Mechatronic Engineering, University of Wollongong, Wollongong, NSW 2522, Australia

**Keywords** Wireless capsule endoscopy · Active anchoring · Magnetic actuation · Legged · Robotic capsule endoscope

## 1 Introduction

Since its advent in 2000 (Iddan et al. 2000), wireless capsule endoscopy (WCE) has been used as a routine procedure to diagnose many gastrointestinal (GI) diseases (Moglia et al. 2009). Current commercial capsules, however, still appear as purely diagnostic devices, though significant efforts have continuously been dedicated to developing relevant modules in order to add interventional and therapeutic functionalities to their diagnostic functionality (Sitti et al. 2015; Koulaouzidis et al. 2015; Alici 2015; Slawinski et al. 2015a, b). Another problem is that current commercial capsules are not capable of monitoring a specific location at a specific time and this causes constraints on the diagnostic functions and makes a follow-on surgical or endoscopic intervention necessary. All these difficulties stem from the fact that current capsules rely on the natural peristalsis for moving inside the GI system, and this cannot be controlled. Therefore, endowing a capsule with movement which is remotely controllable is essential in order to improve the WCE's diagnostic functionality and develop its therapeutic capability.

A number of active locomotion mechanisms have been reported (Moglia et al. 2008; Kim et al. 2010; Valdastrì et al. 2009; Zhou et al. 2013a, b; Kósa et al. 2012). All of these approaches enable the capsules to move independently of the peristalsis. Besides moving, stopping or grounding is the other significant requirement when considering a controllable movement for a WCE. Without the ability to stop the capsule when needed, most promising therapeutic functionalities will not be possible because they all require a capsule to remain at a stable position before initiating interventional procedures

such as biopsy, targeted drug delivery, and/or cauterizing angiectasias. A further advantage of being able to stop the capsule for a prolonged period of time is that longer-term imaging and/or data-collection (e.g., temperature, pH level) at specific sites can be performed and this reduces the possibility of missing information necessary for diagnostic purposes. Some locomotion mechanisms (e.g., inchworm-type, legged-type, etc.) are actually based on repetitive attaching-and-detaching inside the GI tract in order to generate the planned propulsion. The ability to temporarily anchor the locomotion mechanism is essential to make this kind of locomotion mechanism work effectively.

Some anchoring systems have been proposed to operate in various sections of the GI system, i.e. the esophagus (Tognarelli et al. 2009), the stomach (Lien et al. 2012), and the intestine (Glass et al. 2008; Woods and Constandinou 2013). Due to the complex nature of the GI tract (e.g., irregular, slippery, physiologically active, etc.), no conventional methods have been able to provide an endoscopic capsule with long-lasting and effective anchoring onto the intestinal wall without causing bleeding or damage to the GI system (La Spina et al. 2005). So far, most of efforts have been made to develop efficient adhesive materials that suit the feature of the intestinal tissues by mimicking the adhesion mechanisms of some living creatures such as leeches, snails, and geckos (Xie et al. 2015; Dodou et al. 2005; Pensabene et al. 2011; Quaglia et al. 2013; Song et al. 2013). Due to the intestine's rough texture, the high-density fibrillar adhesives significantly increased the contact area. A high coefficient of static friction, 0.35, was reported after measuring the preload forces and the static friction on a porcine intestine (Glass et al. 2008). However, to anchor a WCE, adhesive structures cannot be used on their own because a proper actuation mechanism is also required to attach the adhesives to the intestinal lining and detach them afterwards. Quaglia and the co-workers used a mechanical spring structure to release adhesive patches (Quaglia et al. 2013). The mechanism was triggered by a shape memory alloy wire, which was powered by an onboard battery. Beyond these experiments, the research in this area is very limited. To the best of our knowledge, most anchoring mechanisms reported in the literature use a miniaturized electric motor to open/close anchoring legs, without considering the space consumption in the capsule or the energy consumption. These two very important factors must be taken into account when new modules or additional functions are designed for WCEs.

The purpose of this study is to propose a compact and effective anchoring system for a WCE. In particular, we focus on designing and developing a magnetic actuation system which can remotely provide sufficient preloading force against the natural peristalsis to achieve anchoring in the GI tract. A proof-of-concept capsule was designed and fabricated. *In vitro* tests were conducted by inserting the prototype

capsule with the anchoring mechanism inside a section of a porcine small intestine and these showed the efficacy of the proposed system in anchoring/releasing the capsule at will. This mechanism is low foot-print, not requiring much space or onboard power to endow the existing WCEs with an effective anchoring module. The mechanism works as an add-on module for the capsules and therefore does not require any modification in the current setups (including geometrical and internal arrangements) of WCEs. The proposed mechanism can also be used to establish a robotic capsule with fully controllable locomotion, e.g., an inchworm-like endoscopic robot equipped with such two anchoring mechanisms facilitating the propulsion and subsequently locomotion.

## 2 Design of the anchoring mechanism

Safety is the primary requirement for any medical device. The anchoring mechanism must be reliable and not increase the risk of retention. It must not cause lumen perforation, or any other tissue damage. The second requirement is related to power consumption. A new mechanism needs to be self-powered or externally powered so that the on-board battery can still exclusively provide energy for the basic modules, e.g., vision, signal-transmission, etc. In this regard, magnetic actuation is preferable over an onboard mini electric motor. The third requirement is that the volume should be minimal. The current capsules are usually 11~13 mm in diameter and 24~32 mm in length (Slawinski et al. 2015a, b). Their size and the arrangement of their internal modules are already optimized to meet the volume requirement. Therefore, instead of re-designing and re-arranging the whole capsule to provide the ability to anchor, it is essential to establish an anchoring mechanism which can work as an add-on component for the current capsules. In this way, the existing capsules can easily be given the ability to anchor. To achieve this aim, the anchoring mechanism must not take up too much space so that the whole size of the capsule robot can still be kept small enough for effective operation within the GI tract.

In light of the design requirements described in this section, we propose a leg-type anchoring mechanism coupled with a magnetic actuator which can be remotely operated by an external magnetic field.

### 2.1 Actuation principle

We employ the concept of a magnetic spring (MS) (Simi et al. 2013) to activate the proposed anchoring mechanism. As illustrated in Fig. 1, the MS configuration considered in this study consists of two coaxial ring-shaped permanent magnets (PM)s which are magnetized in the diametrical direction. One of the PMs is free to rotate about their common axis. Without an external magnetic field, the magnets are attracted to each

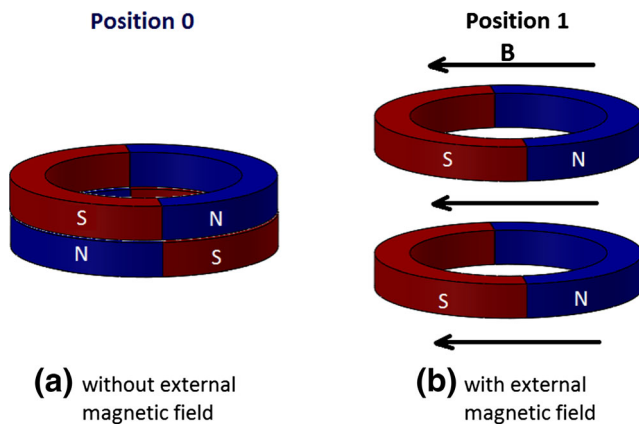


**Fig. 1** Two positions of a switchable magnetic spring

other due to the magnetic dipole-dipole interaction, and remain at this position (calling it Position 0). To pull one PM away from the other in the axial direction, axial forces with an identical magnitude but in the opposite directions need to be applied on both PMs. In this state, the MS acts like a tensile spring with a non-linear pseudo-spring constant. Once the magnets are aligned by an external magnetic field, the attractive force is immediately replaced by a repulsive force because of the same polarity of the magnets in a parallel configuration. The MS suddenly behaves like a compressed mechanical spring, ready to release its mechanical energy. The smaller the gap (as shown in Fig. 1) between the two PMs, the stronger the repulsive force produced on both magnets, which is quite similar to the mechanical behavior of a compressive spring. As soon as the external magnetic field is removed, the MS switches back to a tensile spring and the attractive force brings the magnets together again. Since both the attractive and repulsive forces are the internal forces of an MS, it does not require any constraints from the external environment to support the relative movement between the magnets. In this actuation concept, the orientation of the capsule needs to be known in order to produce an external magnetic field parallel to the magnetization of the permanent magnets, in which the magnetic torque only activates the MS but not changing its capsule's orientation and subsequently twisting the intestine. With the localization method proposed in our previous study (Than et al. 2014a, b), the orientation and position of the capsule can accurately be predicted without interfering with the magnetic actuation.

By utilizing this concept of the switchable magnetic spring, we propose a legged anchoring mechanism to be added on a capsule, as shown in Fig. 2. It is an add-on mechanism for the capsule. Its base is a typical commercial capsule with the dimensions of 11 mm in diameter and 26 mm in length. As can be seen in Fig. 2, PM1 is free to rotate but its linear movement is blocked. At the same time, the rotation of the PM2 is constrained but free to move linearly. Once an external magnetic field is applied, PM2 is repelled away from PM1 and

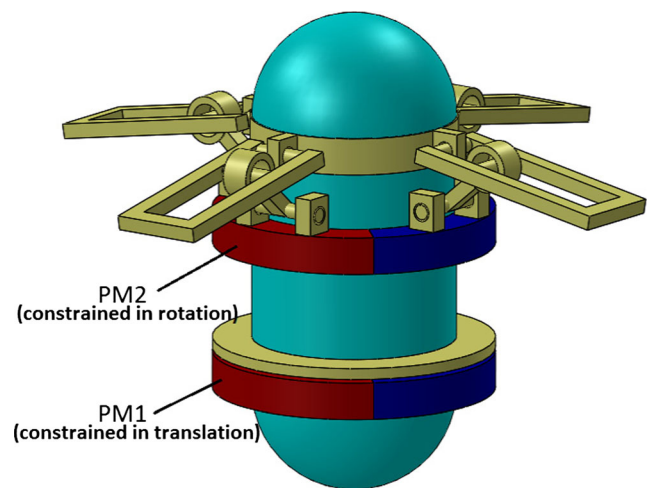


**Fig. 2** A legged anchoring mechanism assembled on an endoscopic capsule

this linear motion opens the legs, which actuates the anchoring mechanism. To detach the capsule, we can simply remove the magnetic field. PM2 will be attracted back to PM1, bringing the legs back to their 'closed' position. The whole capsule is now free to move under the natural peristalsis.

## 2.2 Force analysis

To deploy a capsule inside the GI tract for the desired period of time, the anchoring force must be strong enough to overcome the natural peristalsis and other forces. From the literature (Miftahof 2005), the amplitude of the peristaltic forces for one centimeter length of an object is approximately to be 172 mN in the axial direction and 269 mN in the radial direction. For a commercial capsule with a length of 2.6 cm, the corresponding peristaltic forces are approximately 450 and 700 mN in the axial direction and radial direction, respectively.

For a single leg, its "closed" and "opened" positions are schematically illustrated in Fig. 3(a) and (b), respectively. The leg is comprised of two branches, which are jointed at Point C. Figure 3 shows a half of the upper branch and the lower branch consisting of a folding mechanism with three joints of A, B, and C. The 'soft' half (colored blue in Fig. 3) of the upper branch is made of silicone-like materials such as PDMS providing soft-on-soft contact with the intestinal wall. Once the MS is triggered by an external magnetic field, Point B starts to move upward in the axial direction. With Point A relatively fixed, the whole mechanism depicted in Fig. 3 is 'compressed' in the axial direction but is extended in the radial direction, and this makes the soft component contact the intestinal wall. As it moves, the soft component bends, and this enlarges the contact area between the leg and the intestine. With an adhesive pad attached onto the soft component, a stronger static friction force can be generated to overcome

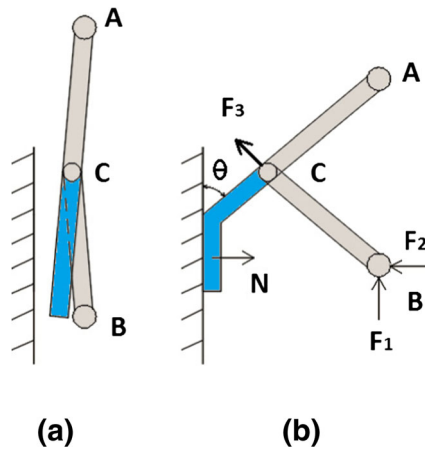


**Fig. 3** Interaction between the leg and the intestinal wall (a) before anchoring; (b) after anchoring

the forces in the GI tract. For anchoring purposes, the combined static friction from the four legs and any other contacting surface of the capsule need to be greater than the total axial peristaltic force.

In Fig. 3(b),  $F_1$  is the repulsive force from the actuated MS.  $F_2$  is the supporting force from the capsule. Hence, for the upper branch, there is  $F_3$ , which is the combination of  $F_1$  and  $F_2$ .  $N$  is the normal force from the intestinal wall. Previous literature (Song et al. 2013) has shown that the coefficient of friction (COF) can reach 0.35 with adhesive pads integrated on the legs. Though it is the combination of the total static friction force that is required to be greater than 450 mN, here we assume that four legs only are responsible for making contact with the intestine in order to generate enough frictional force for anchoring. Hence, each should provide a frictional force  $f = 450/4 = 112.5$  mN. The corresponding normal force from the intestinal wall is  $N = f/\mu = 321$  mN. For the upper branch in Fig. 3, the friction force and the axial peristaltic force offset each other. To consider the moment balance about Point A,  $F_3$  is obtained as:

$$F_3 = \frac{N(2q-d)\sin\theta}{q\sin2\theta} = \frac{N(2q-d)}{2q\cos\theta} \tag{1}$$

where,  $q$  is a half of the upper branch and  $d$  is the bent part of the soft component. Consequently, the magnetic repulsive force on a single leg can be determined from:

$$F_1 = F_3\cos\theta = \frac{N(2q-d)}{2q} \tag{2}$$

From Eq. 2, if the intestine’s diameter is large and there is no bending for the soft component, then the required magnetic force reaches its maximum value, equal to  $N = 321$  mN, for each leg. Therefore, with four legs, the total force requirement from the MS is 1284 mN. This extreme case can be avoided by using a longer or larger soft component when confronting a large intestinal diameter. Since the gastrointestinal tract is soft

and collapsed, the other surface areas of the capsule (e.g., two semispherical ends, etc.) always get in contact with the intestinal wall to some extent and this means that less frictional force from the legs is necessary for anchoring and subsequently less force from the MS for activating the legs.

### 2.3 Magnetic modelling

Using the required magnetic force estimated in the previous section, we select the PMs for the MS to produce enough force. In order to do this, we have conducted a finite element (FE) analysis to quantify the magnetic interaction within a single MS, and determine an acceptable size of the PMs.

According to Ampere’s Law (Jiles 1998)

$$\nabla \times H = J, \tag{3}$$

where  $H$  is the magnetic field intensity and  $J$  is the current density. Equation (3) can be written as

$$\nabla \times \left( \frac{B}{\mu_r\mu_0} \right) = J. \tag{4}$$

The magnetic vector potential  $A$  and the magnetic flux density  $B$  are related with,

$$B = \nabla \times A. \tag{5}$$

Together with the Gauss’s Law of

$$\nabla \cdot B = 0. \tag{6}$$

the governing equation for the magnetostatic solver can be derived as follows,

$$J(x,y,z) = \nabla \times \left( \frac{1}{\mu_r\mu_0} (\nabla \times A(x,y,z)) \right). \tag{7}$$

For  $J(x,y,z)$  given as an excitation, Eq. (7) is solved to obtain the magnetic vector potential  $A$ . The magnetic flux density can then be computed from Eq. (5).

We have used COMSOL software to perform all the FE simulations based on Eqs. (3)–(7). To fit the proposed anchoring mechanism on a standard commercial capsule (11 mm in diameter and 26 mm in length), two magnets are selected with identical dimensions of 11.2 mm internal diameter and 15.2 mm external diameter. Both magnets are diametrically magnetized and their magnetization intensity is equivalent to that of a typical N45 Grade neodymium permanent magnet. Increasing the magnets’ volume is a well-known approach when a stronger magnetic force is required. In our application, instead, we have altered the magnets’ height rather than their diameter because of the capsule robot’s strict diametrical requirement. Three sets of simulations were performed, with different heights (2 mm, 2.5 mm, 3 mm) of the PMs. The magnetic force is calculated between two magnets set in the



range of 1–7 mm. To obtain a repulsive force of  $\sim 1$  N, the distance between the two PMs is approximately 4 mm. In this case, a uniform magnetic field with the intensity of  $\sim 27$  mT is required to produce sufficient magnetic moment to overcome the dipole-dipole coupling of the MS ( $\sim 5$  mNm) and align the permanent magnets. Once the permanent magnets obtain alignment, there exists no magnetic moment anymore no matter how high the external magnetic field is. Therefore, to the functioning of the anchoring mechanism, there is no upper limit for the required external magnetic field. For safety of a human body, the maximum static field strength of 4 T is generally adopted in clinical use (Schenck 2000).

The efficacy of this FE analysis was evaluated experimentally and this is presented in the next section.

### 3 Experiments to validate the magnetic model

To investigate the accuracy of the simulation results and measure the repulsive force generated by an MS, a testing apparatus (see Fig. 4) was designed and constructed using a 3D printer. The MS consists of two neodymium magnets with an inner diameter (ID) of 8.5 mm, outer diameter (OD) of 18.4 mm, thickness of 2 mm and the remanence ( $B_r$ )  $\sim 1.21$  T. As shown in Fig. 4, the ring-shaped permanent magnets were maintained in a co-axial configuration by having a plastic rod (diameter = 8 mm) through their inner diameter. A cap which was placed on top of PM2 was able to move upward along the rod. Once the MS was actuated, the PM2 acquired a repulsive force and pushed the cap up onto the force sensor. The whole testing apparatus was located within a Helmholtz coil system which produced a uniform magnetic field to align the magnetization directions of the PMs and subsequently activate the MS. The electrical current through the coils was gradually raised to increase the intensity of the external magnetic field until the magnetic moment exerted on

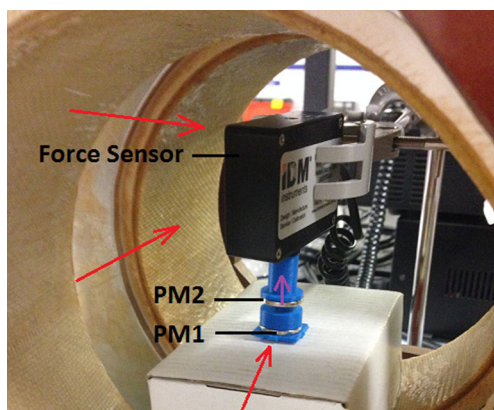


**Fig. 4** A testing apparatus to measure the repulsive force of a magnetic spring (red arrows: indication of the external magnetic field's direction, parallel and through the PMs' diameter; purple arrow: the direction of repulsive force on PM2)

the magnets is strong enough to overcome the dipole-dipole coupling of the MS. Since the external field was uniform, the environment exerted only a magnetic moment on the magnets and had a negligible effect on the force in the vertical direction. The vertical magnetic force was caused almost completely by the magnetic repulsion between two PMs of the MS, which makes it possible to use the force sensor to measure the repulsive force.

The repulsive force of the MS was measured for a set of different gaps between the magnets. Due to the limited power of the electromagnetic system, this distance ranged from 6 to 15 mm. The corresponding magnetic simulations were also obtained using COMSOL. The simulation and experimental results shown in Fig. 5 indicate that the results are reasonably consistent, especially when the gap is relatively large (11 ~ 15 mm). As the gap becomes smaller, the discrepancy between the theoretical and experimental results increases slightly but still remains in the same order of magnitude. With a 6-mm gap between the two magnets, the difference between the FE results and the measurements is only approximately 200 mN. This demonstrates that the FE simulations, which provide an accurate indication of the magnetic force generated by a magnetic spring (MS), can be used for the design and optimization of the MS to be employed in the anchoring mechanism of a capsule endoscope.

### 4 Experiments to validate the feasibility of the prototype anchoring inside a real small intestine

#### 4.1 Experimental setup

To investigate the anchoring ability of the proposed mechanism, a proof-of-concept prototype was designed and fabricated, as shown in Fig. 6. The capsule body is made of acrylonitrile-butadiene-styrene (ABS) and fabricated using a 3D printer (Model: UP Plus 2, Manufacturer: 3D Printing Systems). The four legs providing the anchoring force were

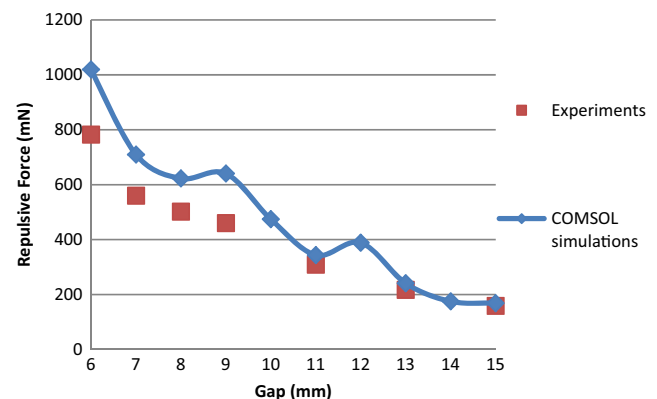


**Fig. 5** Comparison between the FE simulations and the experiments

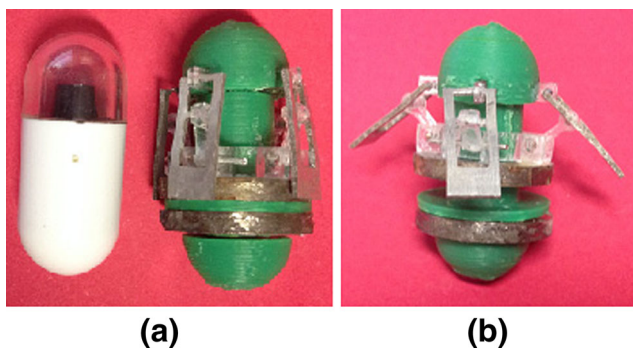


**Fig. 6** (a) The anchoring-type capsule together with a conventional capsule endoscope (PillCam); (b) the anchoring-type capsule with the legs half-opened by an external magnetic field

made of aluminum so that the legs could be thinner (0.5 mm) but stronger than the legs made of the ABS plastic. The legs were cut from a 0.5 mm thick aluminum sheet by using a wire electrical discharge machining (EDM) technique. The diameter of two semi-spherical heads of the capsule is 11 mm and the length of the whole capsule is 28 mm. These dimensions are quite similar to those of the commercial capsules. The section where the PMs are assembled is slightly wider due to the external diameter (15 mm) of the PMs.

The *in vitro* tests were conducted with the capsule moving inside a section of a porcine small intestine. The intestinal specimens, kept in a refrigerator, were unfrozen a few hours before the experiments. Then they were immersed in physiological saline to prevent tissue rupture. The small intestine would dry out quickly once removed from the fluid but the saline could not be sprayed on the intestine segment during the experiment since it would change the frictional properties of the intestine. Therefore, in order to keep the experimental conditions as consistent as possible, each set of tests was finished quickly.

The intestine sample was mounted on a platform which was positioned within a Helmholtz coil system. One end of the capsule was connected to a force sensor to measure the friction force between the capsule and the intestine. For simplicity, the propulsion from the natural peristalsis was usually simulated by externally pulling the capsule when determining the friction inside the intestine *in vitro* (Kim et al. 2006, Glass et al. 2008; Xie et al. 2015). In this study, two approaches were employed to apply an axial pulling force to the capsule. The first one used a stepper motor to apply an axial force and a linear movement to the capsule, as shown in Fig. 7. As reported in the literature (Kim et al. 2006; Zhou et al. 2013a, b, 2014), the sliding friction on tissue is velocity-dependent. With this setup, the capsule moved with a constant speed inside the intestinal tract and only the sliding friction was measured. In the other approach, we replaced the motor with a pulley-weight system to provide a pulling force. In this way, the vertical load which was converted into a horizontal force through the pulley was transferred to the capsule. By

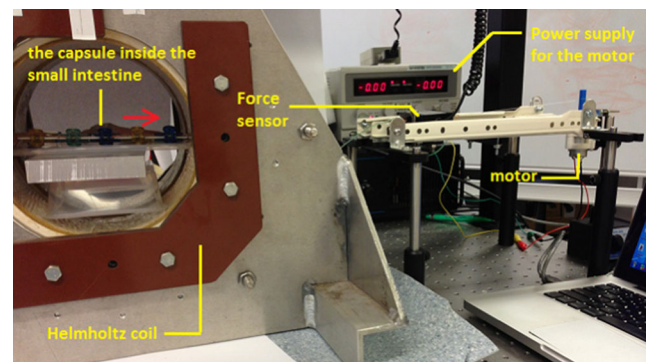


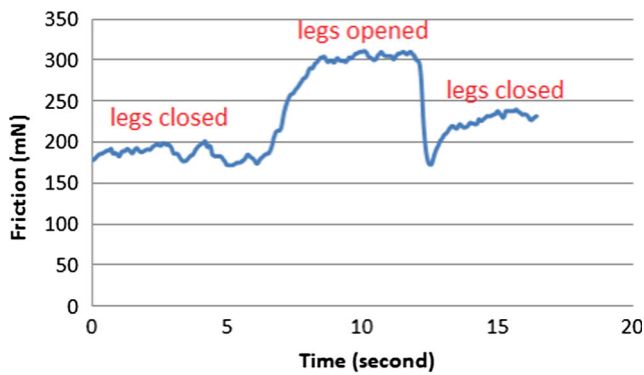
**Fig. 7** The general experimental setup (with a stepper motor); red arrow: moving direction of the capsule

gradually increasing the weight, we recorded the change in the static friction and measured the maximum static friction force as soon as the attachment failed and the capsule started slipping inside the small intestine.

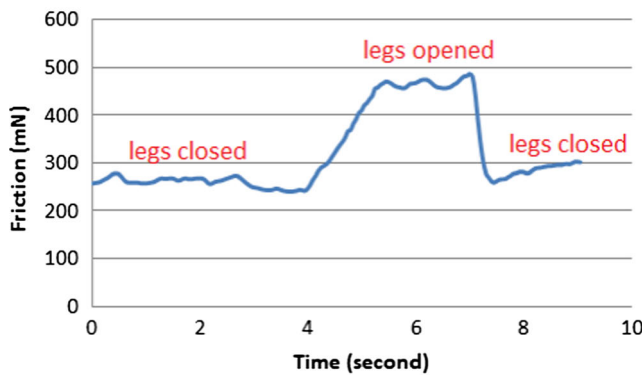
In order to evaluate the performance of the anchoring mechanism, all the force measurements were taken for two states of the capsule: with the legs closed and with the legs opened by switching on/off the external magnetic field.

## 4.2 Experimental results and discussion

The sliding friction of a dummy PillCam SB2 capsule (diameter = 11 mm and length = 26 mm) with a smooth surface was measured first to quantify the effect of adding the anchoring structure on the anchoring force. The measurement was ~85 mN. Figure 8 shows the measurements of the sliding friction force on the legged prototype capsule (shown in Fig. 6) when it was pulled inside the intestine by the stepper motor. The anchoring mechanism was activated in the middle of the linear movement and then deactivated after a few seconds. When the anchoring mechanism turned off, the friction force was approximately 189 mN, which was approximately 2.2 times more than that of a dummy PillCam SB2 capsule. Apparently, having the anchoring structure onboard made the drag force increase, even when the anchoring system was off. However, this impact was not critical because the increased force due to the additional structure was still far smaller than the peristaltic force, which was approximately 450 mN. After turning on the anchoring system, the opened legs stretched the intestine's diameter and exerted more compression onto the intestinal wall, which consequently increased the sliding friction force (seen in Fig. 8(a)). The friction force increased to approximately 300 mN, giving an increase ratio (compared to that with the legs closed) of approximately 1.59. The same experimental procedure was repeated three times. All the results were consistent with an average increase ratio of 1.58. In these tests, the tips of the capsule's legs were pointing in the opposite direction from the movement direction of the capsule.



(a) With the legs' tips pointing opposite to the movement direction of the capsule



(b) With the legs' tips pointing in the movement direction of the capsule

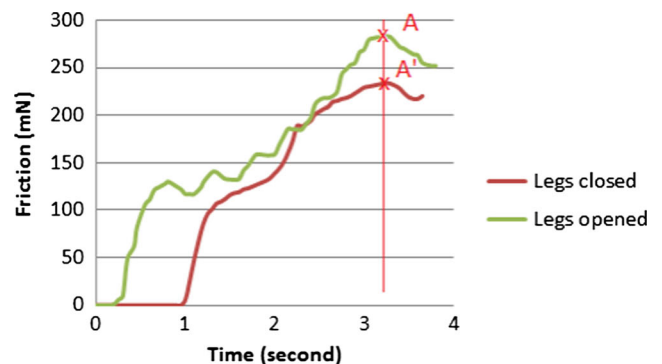
Fig. 8 Friction force measurements for the anchoring mechanism with the capsule pulled by a stepper motor

The second set of tests was carried out immediately after the previous tests with the same intestine sample. In this set of experiments, the capsule moved in the direction from which the tips of the capsule's legs were pointing. The variation in the friction force shown in Fig. 8(b) can be easily seen as the anchoring mechanism was turned on and off. The same procedure was then repeated three times. The average friction forces before and after activating the anchoring mechanism were 222 and 454 mN, respectively. Based on these measurements, the average increase ratio is calculated to be 2.05, which is larger than the one obtained from the previous set of experiments. With the legs' tips pointing in the direction of the movement, the tissue in contact with the tips of the opened legs produced larger drag forces on the capsule and made the anchoring mechanism perform better (i.e. generates more frictional force) in providing a higher anchoring force.

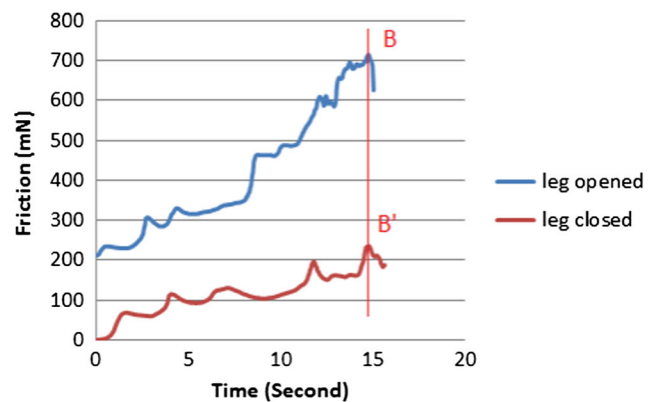
In the following tests, we employed a pulley-weight system to provide an axial force to the capsule instead. A new intestine sample was used. Initially, the capsule stayed still at a specific position inside the intestine. We gradually increased the weight until the capsule started moving so that we could measure the maximum static friction force between the capsule and the intestinal wall.

Figure 9(a) shows the measurements of the static friction force with the legs' tips facing the rear, opposite to the movement direction. The results shown in Fig. 9(a) show that the static friction force gradually increases until it reaches its maximum value (Point A and Point A'). As the weight increased further, the static friction could not increase anymore and it was not strong enough to hold the capsule's position any longer. Therefore, the capsule started to slide and the data beyond Point and Point A' are the measurements of the sliding friction. In Fig. 9(a), it is clearly observed that the capsule exerted a larger static friction force on the intestinal wall with the legs opened by the anchoring system.

The static friction was also measured with the legs' tips facing the front and pointing in the direction of the capsule's movement. Figure 9(b) shows the experimental results. With the anchoring mechanism activated, the opened legs gave rise to a higher reaction force from the intestinal wall and consequently resulted in a higher static friction force acting on the capsule. The maximum static friction force is approximately 700 mN, which is larger than the peristaltic force presented in Subsection 2.2. This indicates a successful stoppage of the capsule endoscope with such an anchoring mechanism.



(a) With the legs' tips pointing opposite to the movement direction of the capsule



(b) With the legs' tips pointing in the movement direction of the capsule

Fig. 9 Friction force measurements for the anchoring mechanism with the capsule pulled by a pulley-weight system



Similar to the sliding friction experiments, the anchoring mechanism generated a higher frictional force against the movement direction of the capsule when the legs' tips point in the direction of movement, compared to that with the legs' tips pointing opposite to the direction of movement.

Table 1 shows a summary of the friction measurements presented above.

To further investigate the performance of the anchoring mechanism, we conducted another test in which the legs were activated first. Then we gradually raised the pulling force to 476 mN, higher than the average peristaltic force predicted. As expected, the capsule remained still due to the higher static friction caused by the opened legs. Considering the viscoelastic nature of the intestine, this position was kept for five minutes and no slippage due to the tissue relaxation was observed. Then we suddenly switched off the electromagnetic system to deactivate the anchoring mechanism. The legs were closed immediately and the capsule failed to overcome the simulated peristaltic force and started moving forward. The series of these actions are shown in the accompanying [video file](#). We repeated the same tests with pulling forces ranging between 450 and 550 mN.

In the further tests, we let the deactivated anchoring mechanism allow the capsule to move under a pulling force. In the middle of the capsule movement, the anchoring mechanism was activated and this successfully stopped the capsule and held its position inside the intestine. After a while, we turned off the anchoring mechanism. Then the capsule was pulled forward again, as illustrated in the accompanying [video file](#).

With all these experimental results, one may argue that *in vitro* condition of a real intestine is different than its *in vivo* condition. It is true that friction measurements from *in vitro* tests were usually slightly larger than those from *in vivo* tests, as reported previously (Lyle et al. 2013). Their study also quantitatively evaluated this difference, showing that the mean value of COF from the *in vivo* tests was approximately 90 % of those from the *in vitro* tests, which was not critical at all since the maximum static friction was measured

to be 700 mN in our study, much more than the peristaltic force of 450 mN. Besides, considering the legs were made of aluminum for this proof-of-concept prototype, there is still room to increase the COF between the contact surfaces by using better materials, such as micro/nano-patterned elastomer adhesive patches (COF  $\sim$  0.35), as introduced in the introduction. As reported by Kim et al., the mean value of COF between an aluminum surface and the intestinal wall was only about 0.09 (Kim et al. 2006).

## 5 Conclusions and future work

In this work, we have proposed a new legged anchoring mechanism for wireless capsule endoscopes by employing the principle of a switchable magnetic spring. A force model is derived to predict the magnetic force required from the magnetic spring. The theoretical analysis and experiments conducted show that the magnetic spring is capable of meeting the anchoring force requirement. Then, a legged anchoring mechanism was designed, fabricated, and assembled onto a capsule with a size comparable to the size of a commercial WCE. The *in-vitro* tests conducted in the samples of a porcine intestine demonstrated that such a capsule could attach to and detach from the intestinal lumen smoothly by switching on and off the external magnetic field, as shown in the accompanying [video files](#). The friction force measurements show that the anchoring mechanism is able to provide more than double the friction, hence providing reliable anchoring for the capsule.

The anchoring legs are made of aluminum with smooth metal surfaces. PDMS pads with micro-sized patterns are reported to significantly increase the coefficient of friction (Glass et al. 2008; Song et al. 2013). Future work will aim to integrate such kinds of bio-inspired adhesives onto the surfaces of the legs and further improve the anchoring ability of this mechanism. Further, a remotely-controlled locking/unlocking mechanism will be developed and added to the

**Table 1** Summary of the friction measurements with or without the anchoring mechanism

Capsule configuration	Intestine sample	Force measurements
Without anchoring mechanism	Sample 1	Sliding friction: 85 mN
With anchoring mechanism (off) and legs' tips pointing opposite to movement direction	Sample 1	Sling friction: 189 mN
With anchoring mechanism (on) and legs' tips pointing opposite to movement direction	Sample 1	Sliding friction: 300 mN
With anchoring mechanism (off) and legs' tips pointing in the movement direction	Sample 1	Sliding friction: 222 mN
With anchoring mechanism (on) and legs' tips pointing in the movement direction	Sample 1	Sliding friction: 454 mN
With anchoring mechanism (off) and legs' tips pointing opposite to movement direction	Sample 2	Maximum Static Friction: 230 mN
With anchoring mechanism (on) and legs' tips pointing opposite to movement direction	Sample 2	Maximum Static Friction: 285 mN
With anchoring mechanism (off) and legs' tips pointing in the movement direction	Sample 2	Maximum Static Friction: 240 mN
With anchoring mechanism (on) and legs' tips pointing in the movement direction	Sample 2	Maximum Static Friction: 700 mN



anchoring system so that the anchoring status can be maintained without keeping the presence of the external magnetic field. With this, the patient does not have to stay with the external electromagnetic system for holding the endoscopic capsule at the specified position, which will dramatically improve the patient compliance and the energy consumption.

**Acknowledgments** This work was supported in part by the Intelligent Nano-Tera Research Systems Laboratory.

The authors wish to gratefully acknowledge the help of Dr. Madeleine Strong Cincotta in the final language editing of this paper.

## References

- G. Alici, Towards soft robotic devices for site-specific drug delivery. *Expert Rev. Med. Devices* **12**, 703–715 (2015)
- D. Dodou, P. Breedveld, P.A. Wieringa, Friction manipulation for intestinal locomotion. *Minim. Invasive Ther. Allied Technol.* **14**, 188–197 (2005)
- P. Glass, E. Cheung, M. Sitti, A legged anchoring mechanism for capsule endoscopes using micropatterned adhesives. *IEEE Trans. Biomed. Eng.* **55**, 2759–2766 (2008)
- G. Iddan, G. Meron, A. Glukhovskiy, P. Swain, Wireless capsule endoscope. *Nature* **405**, 417–418 (2000)
- D. Jiles, *Introduction to magnetism and magnetic materials*, 2nd edn. (Chapman & Hall, London, 1998)
- J.S. Kim, I.H. Sung, Y.T. Kim, E.Y. Kwon, D.E. Kim, Y.H. Jang, Experimental investigation of frictional and viscoelastic properties of intestine for microendoscopy application. *Tribol. Lett.* **22**, 143–149 (2006)
- H.M. Kim, S. Yang, J. Kim, S. Park, J.H. Cho, J.Y. Park, T.S. Kim, E. Yoon, S.Y. Song, S. Bang, Active locomotion of a paddling-based capsule endoscope in an in vitro and in vivo experiment. *Gastrointest. Endosc.* **72**, 381–387 (2010)
- G. Kósa, P. Jakab, G. Székely, N. Hata, MRI driven magnetic microswimmers. *Biomed. Microdevices* **14**, 165–178 (2012)
- A. Koulaouzidis, D.K. Lakovidis, A. Karargyris, E. Rondonotti, Wireless endoscopy in 2020: will it still be a capsule? *World J. Gastroenterol.* **21**, 5119–5130 (2015)
- G. La Spina, C. Stefanini, A. Menciassi, P. Dario, A novel technological process for fabricating micro-tips for biomimetic adhesion. *J. Micromech. Microeng.* **15**, 1576–1587 (2005)
- G.S. Lien, C.W. Liu, J.A. Jiang, C.L. Chuang, M.T. Teng, Magnetic control system targeted for capsule endoscopic operations in the stomach design, fabrication, and in vitro and ex vivo evaluations. *IEEE Trans. Biomed. Eng.* **59**, 2068–2079 (2012)
- A.B. Lyle, B.S. Terry, J.A. Schoen, M.E. Rentschler, Preliminary friction force measurements on small bowel lumen when eliminating sled edge effects. *Tribol. Lett.* **51**, 377–383 (2013)
- R.N. Miftahof, The wave phenomena in smooth muscle syncytia. In *Silico Biol.* **5**, 479–498 (2005)
- A. Moglia, A. Menciassi, P. Dario, Recent patents on wireless capsule endoscope. *Recent Pat. Biomed. Eng.* **1**, 24–33 (2008)
- A. Moglia, A. Menciassi, P. Dario, A. Cuschieri, Capsule endoscopy: progress update and challenges ahead. *Nat. Rev. Gastroenterol. Hepatol.* **6**, 353–362 (2009)
- V. Pensabene, P. Valdastrì, S. Tognarelli, A. Menciassi, A. Arezzo, P. Dario, Mucoadhesive film for anchoring assistive surgical instruments in endoscopic surgery: In vivo assessment of deployment and attachment. *Surg. Endosc. Intervent. Tech.* **25**, 3071–3079 (2011)
- C. Quaglia, S. Tognarelli, E. Sinibaldi, N. Funaro, P. Dario, A. Menciassi, Wireless robotic capsule for releasing bioadhesive patches in the gastrointestinal tract. *J. Med. Devices* **8**, 014503 (2013)
- J.F. Schenck, Safety of strong, static magnetic fields. *J. Magn. Reson. Imaging* **12**, 2–19 (2000)
- M. Simi, G. Gerboni, A. Menciassi, P. Valdastrì, Magnetic torsion spring mechanism for a wireless biopsy capsule. *J. Med. Devices* **7**, 041009 (2013)
- M. Sitti, H. Ceylan, W. Hu, J. Giltinan, M. Turan, S. Yim, E. Diller, Biomedical applications of untethered mobile milli/microrobots. *Proc. IEEE* **103**, 205–224 (2015)
- P.R. Slawinski, K.L. Obstein, P. Valdastrì, Capsule endoscopy of the future: what's on the horizon? *World J. Gastroenterol.* **21**, 10528–10541 (2015a)
- P.R. Slawinski, K.L. Obstein, P. Valdastrì, Emerging issues and future developments in capsule endoscopy. *Tech. Gastrointest. Endosc.* **17**, 40–46 (2015b)
- J. Song, Y. Mengüç, M. Sitti, Enhanced fabrication and characterization of gecko-inspired mushroom-tipped microfiber adhesives. *J. Adhes. Sci. Technol.* **27**, 1921–1932 (2013)
- T.D. Than, G. Alici, S. Harvey, H. Zhou, W. Li, Concept and simulation study of a novel localization method for robotic endoscopic capsules using multiple positron emission markers. *Med. Phys.* **41**, 072501 (2014a)
- T.D. Than, G. Alici, S. Harvey, G. O'Keefe, H. Zhou, W. Li et al., An effective localization method for robotic endoscopic capsules using multiple positron emission markers. *IEEE T Robot.* **30**, 1174–1185 (2014b)
- S. Tognarelli, C. Quaglia, P. Valdastrì, E. Susilo, A. Menciassi, P. Dario, Innovative stop-ping mechanism for esophageal wireless capsular endoscopy. *Procedia Chem.* **1**, 485–488 (2009)
- P. Valdastrì, R.J. Webster, C. Quaglia, M. Quirini, A. Menciassi, P. Dario, A new mechanism for mesoscale legged locomotion in compliant tubular environments. *IEEE Trans. Robot.* **25**, 1047–1057 (2009)
- S.P. Woods, T.G. Constandinou, Wireless capsule endoscope for targeted drug delivery: mechanics and design considerations. *IEEE Trans. Biomed. Eng.* **60**, 945–953 (2013)
- W. Xie, V. Kothari, B.S. Terry, A bio-inspired attachment mechanism for long-term adhesion to the small intestine. *Biomed. Microdevices* **17**, 68 (2015)
- H. Zhou, G. Alici, T.D. Than, W. Li, Modeling and experimental characterization of propulsion of a spiral-type microrobot for medical use in gastrointestinal tract. *IEEE Trans. Biomed. Eng.* **60**, 1751–1759 (2013a)
- H. Zhou, G. Alici, T.D. Than, W. Li, Modeling and experimental investigation of rotational resistance of a spiral-type robotic capsule inside a real intestine. *IEEE-ASME Trans. Mechatron.* **18**, 1555–1562 (2013b)
- H. Zhou, G. Alici, T.D. Than, W. Li, Experimental investigation into biomechanical and biotribological properties of a real intestine and their significance for design of a spiral-type robotic capsule. *Proc. IMechE, Part H: J. Eng. Med.* **228**, 280–286 (2014)